The Paramagnetic Ground State of Ruby—Revisited

J. Shell[1]

A more accurate formula for the ruby spin Hamiltonian (than used in earlier JPL programs) is presented for calculating the ground-state paramagnetic spectrum of ruby and transition probability matrix elements between quantum states induced by radio-frequency magnetic fields. A coordinate system is chosen that simplifies the expressions for the radio-frequency magnetic field. Applications of the computer program to several past and current Deep Space Network maser designs are presented. The program is included in an appendix along with a sample output.

I. Introduction

The low-noise maser amplifiers in the Deep Space Network (DSN) use ruby as the active material. The quantum states of the paramagnetic chromium ion in the ruby crystal are used in the amplification process. An external static magnetic field, $\overrightarrow{H_{dc}}$, is applied to the ruby to generate the quantum states. The nature of these states depends on the strength and orientation of this field relative to the ruby crystal c-axis. Transitions between these quantum states are induced by radio frequency (rf) magnetic fields. These transitions are used in two distinct ways. In the first instance, microwave energy from a pump source is used to alter the distribution of spins amongst the energy levels. This creates the population inversion necessary for the ruby to amplify an incoming signal. In the second instance, the process of stimulated emission amplifies the transitions resulting from an incoming "signal." This incoming signal may be from a distant spacecraft, for example.

A good model and understanding of the ruby's paramagnetic behavior are necessary for maser design. In particular, the low-lying energy levels, which are used in cryogenic low-noise amplifiers, are of interest. The ability to calculate the transitions between levels induced by an rf field is also necessary for good maser design. This article contains a computer program that models these effects. The program can be used to select static magnetic-field strengths and orientations and microwave magnetic-field orientations and polarization. This program can aid in the understanding of current and past DSN ruby masers.

In 1970, a Fortran program was written to calculate these same quantities using a different coordinate system and different numerical values for the parameters used to describe the ruby [1]. This program was used to generate many sets of tables for maser design. Some tables exist today, but the program is no longer readily available. In 1978, the National Bureau of Standards (NBS) published a report describing the use of ruby as a standard reference material in electron paramagnetic resonance experiments [2]. It published precise values of the spectroscopic splitting factors and the zero-field splitting for ruby.

---

[1] Communications Ground Systems Section.

The research described in this publication was carried out by the Jet Propulsion Laboratory, California Institute of Technology, under a contract with the National Aeronautics and Space Administration.

The program described in this article uses these more recent values. The program also uses a different coordinate system that simplifies the task of calculating transition probabilities due to an rf field. Rather than aligning the ruby crystal c-axis in the z-direction, the applied static magnetic field is chosen along the z-direction [3]. In addition, the advent of new commercial software specifically designed to work with matrices allows for a much simpler program [4]. The program listing and a sample output are included in Appendix A.

II. Spin Hamiltonian for Ruby

A very concise description of the low-lying states, often referred to as the ground state, is made possible through the concept of an effective spin Hamiltonian. This approach includes such effects as the Zeeman splitting of the states due to applied magnetic fields, including anisotropy of this splitting. It also describes the splitting of energy levels due to the electrostatic field of surrounding atoms. In the case of ruby, this appears as a quadrupole interaction. Excellent discussions of this concept can be found in several books [5,6].

The presence of the crystal field makes the form of the Hamiltonian dependent on the orientation of the coordinate system. For example, if the ruby crystal c-axis is chosen along the z-direction, then the spin Hamiltonian, H_s, is given by

$$H_s = g_1 \beta H_z S_z + g_2 \beta (H_x S_x + H_y S_y) + D \left[S_z^2 - \frac{1}{3} S(S+1) \right] \tag{1}$$

Here, g_1 and g_2 are spectroscopic splitting factors, β is the Bohr magneton, and $\overrightarrow{H_{dc}} = (H_x, H_y H_z)$ is the applied static magnetic field. The spin vector is denoted by $\overrightarrow{S} = (S_x, S_y, S_z)$. Here, S_x, S_y, S_z are spin matrices, given below. The variable D represents one half of the zero-field splitting between the $S_z = \pm 1/2$ spin states and the $S_z = \pm 3/2$ spin states. The quantity $S(S+1)$ is the eigenvalue of the operator $S^2 = S_x^2 + S_y^2 + S_z^2$. Equation (1) is very similar to the expression used in [1]. The coordinate system appropriate to this form is shown in Fig. 1(a).

Personnel at Bell Telephone Laboratories used a Hamiltonian wherein the z-axis is along the applied static magnetic field [3]. The ruby crystal c-axis is specified by the polar angle, θ, with respect to the dc magnetic field and an azimuthal angle, φ, with respect to the x-axis. Their result is

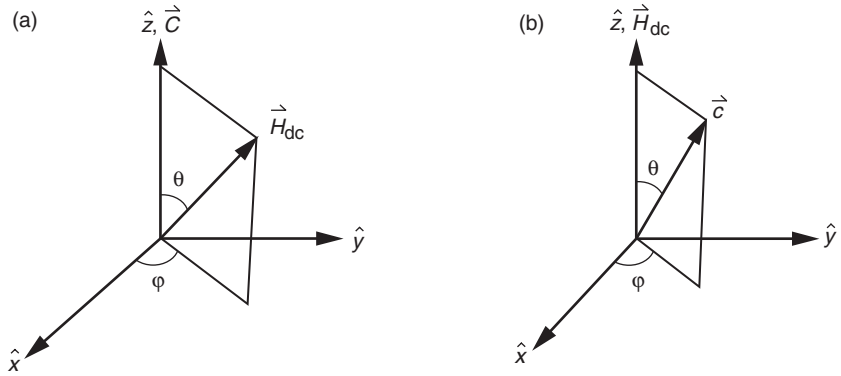

Fig. 1. The coordinate system used in (a) Eq. (1) and (b) Eq. (2).

$$
\begin{aligned}
H_s = {} & (g_1 \cos^2\theta + g_2 \sin^2\theta)\beta H_z S_z \\
& + D\left(\cos^2\theta - \frac{1}{2}\sin^2\theta\right)\left[S_z^2 - \frac{1}{3}S(S+1)\right] \\
& + D\left(\frac{1}{2}\right)(\cos\theta\sin\theta)\left[e^{-j\varphi}\left(S_z S_+ + S_+ S_z\right) + e^{j\varphi}\left(S_z S_- + S_- S_z\right)\right] \\
& + D\left(\frac{1}{4}\right)\sin^2\theta\left(e^{-2j\varphi}S_+^2 + e^{2j\varphi}S_-^2\right)
\end{aligned}
\tag{2}
$$

Here, $S_+ = S_x + jS_y$, $S_- = S_x - jS_y$, and $j = \sqrt{-1}$. We use the values for the spectroscopic splitting factors $g_1 = 1.9817$ and $g_2 = 1.9819$, and the zero-field splitting $D = -3.8076 \times 10^{-17}$ ergs, published by the National Bureau of Standards. This is the form that will be used for the results presented in this article.

The coordinate system appropriate to the Hamiltonian of Eq. (2) is shown in Fig. 1(b). From the point of view of the crystal, it's a more natural choice to choose the z-axis along the c-axis direction. From the point of view of the rf magnetic fields, it makes more sense to let the direction of the c-axis be unrestricted. The result is a more complex expression for the spin Hamiltonian. However, since a digital computer performs the calculation, the additional complexity is not a concern. Equation (2) can be shown to be almost exactly equal to Eq. (1). We have neglected terms involving the difference between g_1 and g_2 because they are nearly equal. Demonstration of the equivalence is discussed in Appendix B.

The values predicted by this program are different from the values published by Berwin [1] or Siegman [6]. This is due to the slightly different values of the spectroscopic splitting factor and zero-field splitting used by the two programs. For example, with a 2600-gauss magnetic field oriented 90 degrees to the ruby c-axis, Berwin calculates the 1–2 transition frequency to be 2.6083 GHz. The current program predicts 2.5677 GHz, a difference of 40.6 MHz, or about 1.5 percent.

In addition to choosing a coordinate system, we must choose a representation for the spin operators. This means choosing a set of base states in terms of which the spin quantum states can be expressed. The usual choice for a spin system is the set of states that are simultaneous eigenstates of the total angular momentum squared and the projection of the angular momentum along some axis, usually the z-axis. In this representation, the matrices representing S^2 and S_z are diagonal. We also adopt this convention. For a spin $S = 3/2$ system, such as the Cr^{+3} ion in ruby, S^2 and S_z are given by $(2S+1)$-by-$(2S+1)$ matrices. In particular,

$$
\begin{aligned}
S^2 &= \frac{15}{4} \cdot \begin{bmatrix} 1 & 0 & 0 & 0 \\ 0 & 1 & 0 & 0 \\ 0 & 0 & 1 & 0 \\ 0 & 0 & 0 & 1 \end{bmatrix} \\
S_z &= \frac{1}{2} \cdot \begin{bmatrix} 3 & 0 & 0 & 0 \\ 0 & 1 & 0 & 0 \\ 0 & 0 & -1 & 0 \\ 0 & 0 & 0 & -3 \end{bmatrix}
\end{aligned}
\tag{3a}
$$

In this representation, the matrices representing the spin operators S_x and S_y are given by

$$S_x = \frac{1}{2} \cdot \begin{bmatrix} 0 & \sqrt{3} & 0 & 0 \\ \sqrt{3} & 0 & 2 & 0 \\ 0 & 2 & 0 & \sqrt{3} \\ 0 & 0 & \sqrt{3} & 0 \end{bmatrix}$$

$$S_y = \frac{1}{2} \cdot \begin{bmatrix} 0 & -\sqrt{3}j & 0 & 0 \\ \sqrt{3}j & 0 & -2j & 0 \\ 0 & 2j & 0 & -\sqrt{3}j \\ 0 & 0 & \sqrt{3}j & 0 \end{bmatrix} \tag{3b}$$

From Eqs. (1) or (2) and (3), it can be seen that the spin Hamiltonian is a 4-by-4 matrix. The eigenvalues of the matrix are the energies of the discrete quantum states available to the spins. The difference in energies divided by Planck's constant determines the resonant transition frequencies. The eigenvector associated with an eigenvalue is a representation of the quantum state having that energy. The transition frequencies are calculated and displayed by the program. The eigenvectors are used to calculate the spin vectors discussed in the next section. The eigenvectors are not normally displayed, although it is a simple matter to do so.

III. Transition Probability Matrix Elements and Spin Vectors

The ability of the rf magnetic field to induce transitions between the quantum states of ruby is fundamental to maser design. If the rf field is the signal from a spacecraft, this ability is related to the gain of the maser. If the rf field is from a microwave pump source, this ability is related to the amount of pump energy needed to saturate the transition. A measure of the ability of a given rf field to induce a transition is given by a matrix element.

The transition probability between quantum states i and j induced by an rf magnetic field is

$$W_{i \to j} = \frac{1}{4}\gamma^2 g(f) \left| \left\langle j \right| \overrightarrow{H^*_{rf}} \cdot \vec{S} \left| i \right\rangle \right|^2 \tag{4}$$

where $\gamma = g\beta\mu_o/\hbar$ and $g(f)$ is the line-shape function. The matrix element mentioned above is given by $\langle j| \overrightarrow{H^*_{rf}} \cdot \vec{S} |i\rangle$. The quantum states, $\langle j|$, $|i\rangle$, are represented by the eigenvectors of the spin Hamiltonian. The spin vector is shorthand for $\vec{S} = (S_x, S_y, S_z)$, where the spin matrices are given above.

As seen in Eq. (4), the operator describing the interaction between the spin and the rf magnetic field has much the same form as the operator describing a spin in a static magnetic field. It takes the form of a dot product between the conjugate of the rf magnetic field vector and the spin vector. The magnetic field vector can be pulled outside the brackets, leading to the expression

$$\overrightarrow{H^*_{rf}} \cdot \left\langle j \right| \vec{S} \left| i \right\rangle = \overrightarrow{H^*_{rf}} \cdot \left\{ \langle j|S_x|i\rangle \, \hat{x} + \langle j|S_y|i\rangle \, \hat{y} + \langle j|S_z|i\rangle \, \hat{z} \right\}$$

$$= H^*_x \cdot S^{ij}_x + H^*_y \cdot S^{ij}_y + H^*_z \cdot S^{ij}_z = \overrightarrow{H^*_{rf}} \cdot \overrightarrow{S^{ij}}$$

In general, $H^*_x, S^{ij}_x, H^*_y, S^{ij}_y, H^*_z, S^{ij}_z$ are complex numbers. Thus, the transition probability between two states depends on the magnitude, orientation, and polarization of the rf magnetic field. The spin vectors, $\overrightarrow{S^{ij}} = \langle j| \vec{S} |i\rangle$, as well as the quantities $T_{ij} = \left| \overrightarrow{H^*_{rf}} \cdot \overrightarrow{S^{ij}} \right|^2$, for a user-specified rf field, are calculated by the program.

IV. Program Description and Examples Using the Program

The program is written in the high-level language MATLAB. This is commercial software specifically designed to handle matrices. MATLAB has intrinsic eigenvalue and eigenvector routines. This greatly reduces the program length. After the Hamiltonian is entered into the program, the eigenvalues and eigenvectors are calculated by executing one statement. The eigenvectors are ordered with the one corresponding to the lowest energy, e_1, labeled v_1, and the next one labeled v_2, and so on. The eigenvectors calculated by MATLAB are also orthogonal and normalized. For a general choice of the azimuth angle, φ, the eigenvectors are complex. If the c-axis is chosen in the x–z plane, that is, $\varphi = 0$ or 180 degrees, the eigenvectors are real.

The program input consists of the static magnetic-field strength, the angles θ and φ specifying the c-axis orientation and the rf magnetic field in phasor form. The program calculates and displays the transition frequencies (in GHz), the associated spin vectors, and the quantity T_{ij} for all the transitions. A sample output follows the program listing.

The user can check the transition frequencies for selected field strength and orientation against the NBS tables. The NBS tables include values for $T_{x'}^{\alpha\beta} = |\langle\alpha| S_{x'} |\beta\rangle|^2$ and $T_{y'}^{\alpha\beta} = |\langle\alpha| S_{y'} |\beta\rangle|^2$. These can be compared against the T_{ij} calculated by the program by entering $H_{rf} = (1, 0, 0)$ and $H_{rf} = (0, 1, 0)$, respectively, as program input. Note that the levels in the NBS tables are labeled in the opposite order, with level 1 being the highest and level 4 being the lowest.

In the following subsections, the program is used to analyze or describe past and current DSN masers.

A. Example 1: S-Band Coaxial Cavity Masers

Our first example of the use of the program will be a comparison of two early 2.36-GHz (S-band) coaxial cavity masers. The first such cavity had the ruby oriented in the coaxial line, as shown in Figs. 2(a) and 2(b).[2] The static magnetic field was oriented perpendicular to the coaxial line. Its strength was approximately 2500 gauss. The rf magnetic-field lines of constant magnitude are circles surrounding the center conductor in a plane perpendicular to the center conductor, as shown in Fig. 2(c). The ruby c-axis is in a plane perpendicular to the static magnetic field and oriented 30 degrees out of the plane of the rf magnetic field.

With the right-hand x–y–z coordinate system in Fig. 2(a), we set $\varphi = 60$ degrees and $\theta = 90$ degrees. The rf-field lines of constant magnitude form circles in the y–z plane, and the polarization is linear. The

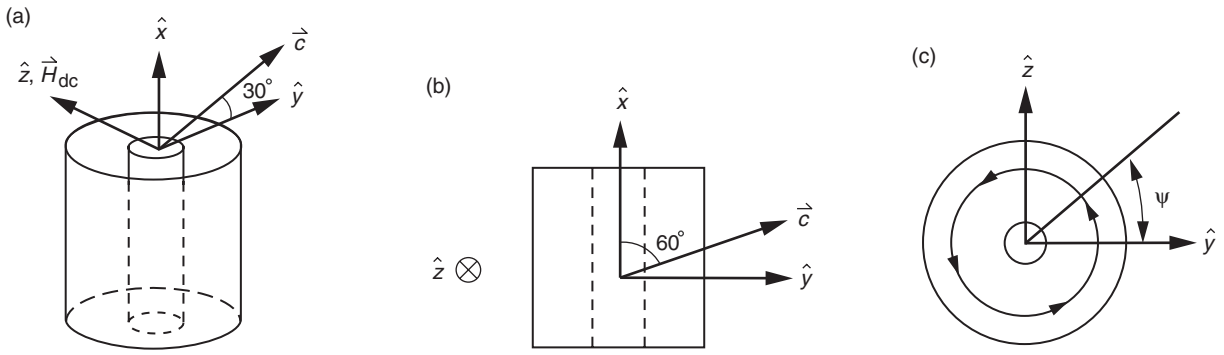

Fig. 2. The first S-band coaxial cavity: (a) a perspective drawing showing the direction of the static magnetic field and the crystal c-axis, (b) a side view, and (c) a top view (a typical rf magnetic field line is also shown).

[2] R. C. Clauss, personal communication, Jet Propulsion Laboratory, Pasadena, California, February 2002.

interaction of the ruby with the linear rf field depends on the angle ψ, shown in Fig. 2(c). We can generate a table of transition probabilities as a function of ψ by changing the relative magnitude of the y- and z-components of the rf magnetic field. Because of the symmetry, we need only cover 1/4 of the circumference of the circle. We choose 10-degree increments.

A word about our notation is in order. We will represent the rf magnetic field in the form $H_{rf} = H_1(a, b, c)$, where a, b, c can be complex and satisfy $|a|^2 + |b|^2 + |c|^2 = 1$. In its most general form, H_1 would be $H_1 = he^{j\alpha}$. The actual rf field is given by multiplying H_{rf} by $e^{j\omega t}$ and taking the real part. In our examples, H_1 will be chosen equal to one. For example, a right-hand circular polarized wave in the x–y plane would be written as $H_{rf} = (1, -j, 0)$. If the wave is viewed as propagating toward the observer, then if the fingers of the right hand curl in the direction of vector rotation, the thumb will point toward the observer. The linear rf field phasors are listed in Table 1 along with the associated value of T_{12}. For the 1–2 transition, the average value of T_{12} per unit rf field strength is $T_{12}/H_1 = 0.623$.

To accurately estimate the ruby absorption, we would have to account for the stronger field near the shorted end of the ruby cavity, as well as the variation of the field strength from the center conductor to the outer conductor. Since the second maser geometry in this comparison is the same as the first, we will neglect these effects. The second maser geometry is shown in Figs. 3(a) and 3(b) [7]. Now the static magnetic field is along the center conductor of the coaxial line, and the ruby c-axis is in the plane perpendicular to it. It is also the plane of the rf magnetic field, as seen in Fig. 3(c). For this orientation, we set $\theta = 90$ degrees and $\varphi = 0$ degrees. Again we vary H_{rf}, at 10-degree increments, around 1/4 of the circumference of the circle in the x–y plane. The transition probabilities are shown in Table 2. For the 1–2 transition, the average value of T_{12} per unit rf field strength is $T_{12}/H_1 = 0.892$. Therefore, the second maser geometry should be significantly better, with a transition probability for the signal transition about 43 percent greater than the first geometry.

B. Example 2: X-band Coupled-Cavity Maser

The next example concerns the behavior of ruby as it might appear in a DSN 8.42-GHz (X-band) coupled-cavity maser. This is shown schematically in Fig. 4. The ruby crystal is shown in a cavity with a signal broadbanding cavity on the left and a pump broadbanding cavity on the right. To the left of the signal broadbanding cavity is a stepped-height pump reject filter. An applied static magnetic

Table 1. First S-band coaxial cavity.

H_{rf}	T_{12}
(0, 1, 0)	1.2451
(0, 0.985, 0.174)	1.2081
(0, 0.949, 0.342)	1.1002
(0, 0.866, 0.500)	0.9338
(0, 0.766, 0.643)	0.7306
(0, 0.643, 0.766)	0.5148
(0, 0.500, 0.866)	0.3113
(0, 0.342, 0.940)	0.1456
(0, 0.174, 0.985)	0.0377
(0, 0, 1)	0.0
—	0.623 (average)

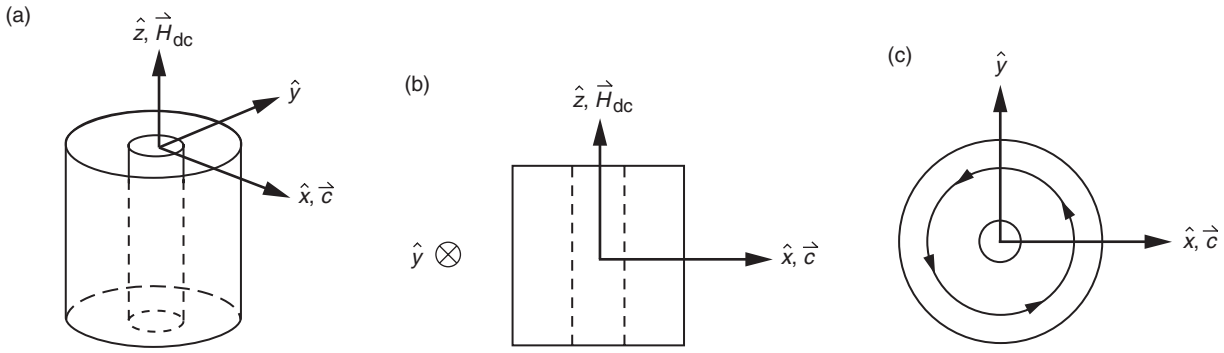

Fig. 3. The second S-band coaxial cavity: (a) a perspective drawing showing the direction of the static magnetic field and the crystal c-axis, (b) a side view, and (c) a top view (a typical rf magnetic field line is also shown).

Table 2. Second S-band coaxial cavity.

H_{rf}	T_{12}
(1, 0, 0)	1.5985
(0.985, 0.174, 0)	1.5565
(0.949, 0.342, 0)	1.4341
(0.866, 0.500, 0)	1.2451
(0.766, 0.643, 0)	1.0144
(0.643, 0.766, 0)	0.7695
(0.500, 0.866, 0)	0.5384
(0.342, 0.940, 0)	0.3505
(0.174, 0.985, 0)	0.2280
(0, 1, 0)	0.1851
—	0.892 (average)

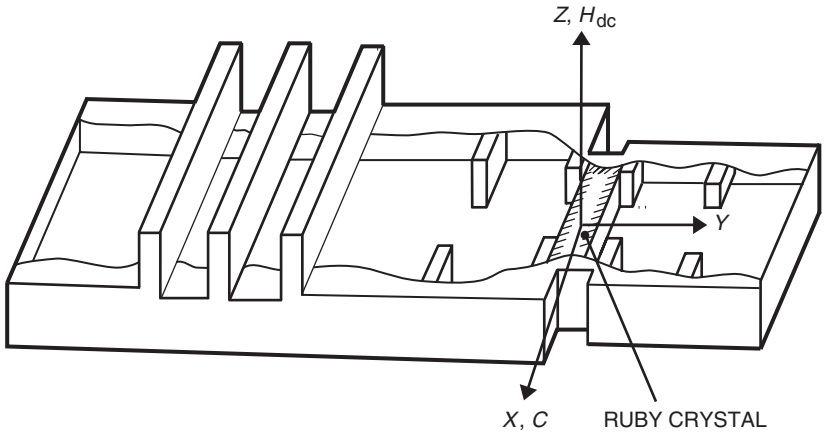

Fig. 4. A perspective view of an X-band coupled-cavity maser. The cavities are drawn for illustrative purposes only; they are not to scale.

field of 4,981 gauss is oriented 90 degrees to the crystal c-axis. The signal transition is chosen between levels 1 and 2 and occurs at 8.421 GHz. The first pump transition is between levels 1 and 3 and occurs at 24.05 GHz. A second pump transition is between levels 3 and 4 and occurs at 19.21 GHz. The spin vectors for these transitions are very important to the maser design.

The spin vector for the signal transition is $\overrightarrow{S_{12}} = (-1.0735, 0.65443j, 0)$. Since we have chosen $\varphi = 0$, the c-axis is in the x-direction. Thus, if the rf fields of the signal are linearly polarized, as in the case of the coupled-cavity maser, the interaction with the ruby is stronger if the rf magnetic field is predominantly in the x-direction rather than the y-direction. The value of T_{12} with $H_{rf} = (1, 0, 0)$ is 1.1525. The value of T_{12} with $H_{rf} = (0, 1, 0)$ is 0.4282. Thus, the advantage is 2.69. Therefore, elongating the cavity in the x-direction will increase the coupling with the rf magnetic field. From this we can also see that rf magnetic fields in the z-direction, along the applied static magnetic field, are ineffective in inducing transitions.

The spin vector indicates that the optimum rf field polarization is elliptical. If an rf field of unit amplitude is linearly polarized in the x-direction, then $T_{12} = 1.1524$. That is the best you can do with a linearly polarized signal. However, if the rf field has the proper elliptical polarization and is of unit amplitude, then $H_{rf} = (0.854, -0.521j, 0)$ and $T_{12} = 1.582$. There also exists an rf field polarization in this plane that does not induce a response. It is $H_{rf} = (0.521, 0.854j, 0)$.

The spin vector for the first pump transition is $\overrightarrow{S_{13}} = (0, 0, 0.4140)$. Thus, a linearly polarized field in the z-direction will be required to stimulate this transition. Therefore, the pump waveguide feeding the ruby cavity must support a 24-GHz mode whose electric field is perpendicular to the applied magnetic field. Finally, the spin vector for the second pump is $\overrightarrow{S_{34}} = (-0.7229, 1.0051j, 0)$. It is similar to the signal component, except the roles of the x- and y-directions are reversed. The value of T_{34} with $H_{rf} = (1, 0, 0)$ is 0.5225. The value of T_{34} with $H_{rf} = (0, 1, 0)$ is 1.0102. Now the transition probability is almost twice as strong for the linear rf field polarized in the y-direction as compared to the x-direction.

C. Example 3: Ka-Band Coupled-Cavity Maser

Our last example will concern the behavior of ruby as it is used in the current DSN 31.8- to 32.3-GHz (Ka-band) coupled-cavity maser. This is shown schematically in Fig. 5. A static magnetic field of 11,881 gauss is applied along the z-direction, and the ruby c-axis is oriented 54.735 degrees to this direction. The signal transition occurs between levels 2 and 3 at frequencies around 32 GHz. The spin vector for this transition is $\overrightarrow{S} = (-0.9777, 0.9786j, -0.0424)$. Therefore, for maximum transition probability, the rf magnetic field should be $H_{rf} = (0.707, -0.707j, 0.031)$. This is a circularly polarized

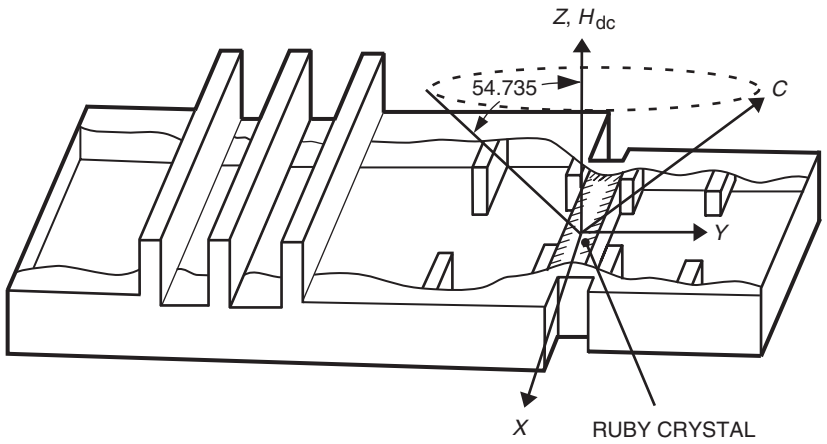

Fig. 5. A perspective view of a Ka-band coupled-cavity maser. The cavities are drawn for illustrative purposes only; they are not to scale.

signal in the x–y plane. For this reason, the orientation of the c-axis in azimuth is not important. The c-axis can lie anywhere on a cone at 54.735 degrees to the applied field without affecting the signal transition probability.

Two pump transitions typically are used for this operating point. The first pump between levels 1 and 3 occurs at 66.25 GHz. The spin vector for this transition is $\overrightarrow{S} = (-0.1455, 0.1519j, 0.0990)$. For maximum transition probability, the rf magnetic field should be $\overrightarrow{H_{rf}} = (0.6259, -0.6534j, -0.4259)$. This is nearly a circularly polarized signal in the x–y plane, with a significant, but smaller, component in the z-direction. For this reason, this transition normally is pumped with waveguide modes whose electric fields lie along the applied static magnetic field.

The second pump between levels 2 and 4 also occurs at 66.25 GHz. The spin vector for this transition is $\overrightarrow{S} = (-0.1289, 0.1183j, 0.0990)$. Therefore, for maximum transition probability, the rf magnetic field should be $\overrightarrow{H_{rf}} = (0.6399, -0.5873j, -0.4955)$. This is more elliptical than the first pump, but the difference between T_{24} for an x-polarized rf field and a y-polarized rf field is never more than 17 percent as the c-axis is varied in azimuth. Again, the z-component is smaller than either the x- or y-component. The waveguide modes mentioned above are also used for pumping this transition. It is a fortunate situation that pump energy at the same frequency and in the same waveguide mode is effective in pumping both transitions. This is especially helpful at this operating point where the pump transitions are very weak. If $H_{rf} = (0.7071, 0.7071, 0)$, $T_{13}/T_{23} = 0.023$ and $T_{24}/T_{23} = 0.016$. This is the main reason for having the ruby cavity resonant at both the signal and pump frequencies in the coupled-cavity maser design.

V. Conclusion

A program has been written to calculate the ground state spectrum of ruby and the transition probability due to an rf magnetic field. This information is used in the design and analysis of masers using ruby as the active material. It is based on a Hamiltonian where the z-axis is along the static magnetic field and the x- and y-axes are chosen to simplify the expressions for the rf magnetic field. The direction of the c-axis is specified by two polar angles. It is written in the language of MATLAB and is included in Appendix A for reference purposes. A discussion of some DSN masers using the results of the program is presented.

References

[1] R. Berwin, *Paramagnetic Energy Levels of the Ground State of Cr^{+3} in Al_2 O_3 (Ruby)*, Technical Memorandum 33-440, Jet Propulsion Laboratory, Pasadena, California, January 15, 1970.

[2] T. Chang, D. Foster, and A. H. Kahn, "An Intensity Standard for Electron Paramagnetic Resonance Using Chromium-Doped Corundum (Al_2O_3:Cr^{3+})," *Journal of Research of the National Bureau of Standards*, vol. 83, no. 2, pp. 133–164, March–April 1978.

[3] E. O. Schulz-Du Bois, "Paramagnetic Spectra of Substituted Sapphires—Part I: Ruby," *Bell System Technical Journal*, vol. 38, p. 271, January 1959.

[4] MATLAB, Version 5, The MathWorks, Inc., Natick, Massachusetts, copyright 1984–1998.

[5] A. Abragam and B. Bleaney, *Electron Paramagnetic Resonance of Transition Ions*, New York: Dover Publications, Inc., 1986.

[6] A. E. Siegman, *Microwave Solid State Masers*, New York: McGraw-Hill Book Company, 1964.

[7] R. C. Clauss, "A 2388 Mc Two-Cavity Maser for Planetary Radar," *Microwave Journal*, May 1965.

Appendix A

Ruby Energy Level Program and Sample Output

The MATLAB program listing follows. Statements following a "%" are comments. (Notice that MATLAB denotes $\sqrt{-1}$ by i.)

```
% an m-file called rubylevels.m to calculate the eigenvalues
% and eigenvectors of the spin hamiltonian for ruby
% it calculates the spin vector and the transition frequencies (in GHz)
% and also the transition probabilities for a given r-f magnetic field
% Hdc is along the z-axis and the c-axis direction is unrestricted

g1=1.9817;              % use the values for g1, g2 and D
g2=1.9819;              % suggested by the National Bureau
D=-3.8076e-17;          % of Standards
beta=9.273e-21;

h=4981              % enter the magnetic field strength
thetad=90.0         % enter the polar angle
phid=0.0            % enter the azimuthal angle
Hrf=[0.854; -0.521i; 0.0]       % enter the r-f field polarization

theta=pi*(thetad/180.0);        % convert polar angle to radians
phi=pi*(phid/180.0);            % convert azimuthal angle to radians

% construct the spin hamiltonian
Sx=(0.5)*[0 1.732 0 0;1.732 0 2 0;0 2 0 1.732;0 0 1.732 0];
Sy=(0.5)*[0 -1.732i 0 0;1.732i 0 -2i 0;0 2i 0 -1.732i;0 0 1.732i 0];
Sz=(0.5)*[3 0 0 0;0 1 0 0;0 0 -1 0;0 0 0 -3];
Sp=Sx+i*Sy; Sm=Sx-i*Sy;
sh1=(g1*(cos(theta))^2+g2*(sin(theta))^2)*beta*h*Sz;
sh2=D*((cos(theta))^2-(0.5)*(sin(theta))^2)*(Sz^2-1.25*eye(4));
sh3=D*(sin(theta))*(cos(theta))*(0.5)*exp(-i*phi)*(Sz*Sp+Sp*Sz);
sh4=D*(sin(theta))*(cos(theta))*(0.5)*exp(i*phi)*(Sz*Sm+Sm*Sz);
sh5=D*(0.25)*(sin(theta))^2*(exp(-2*i*phi)*Sp^2+exp(2*i*phi)*Sm^2);
sh=sh1+sh2+sh3+sh4+sh5;

% calculate the eigenvectors and eigenvalues
[evect,eval]=eig(sh);
e1=eval(1,1); e2=eval(2,2); e3=eval(3,3); e4=eval(4,4);
% the eigenvector associated with the first eigenvalue is the first
% column of the matrix evect, the 2nd eigenvector is the 2nd column, etc
v1=evect(:,1); v2=evect(:,2); v3=evect(:,3); v4=evect(:,4);

% order the eigenvalues such that the most negative one is labeled e1
% and the most positive one is labeled e4, carry the eigenvectors
% along with the eigenvalues
if  e1>e2
   et=e1;    vt=v1;
   e1=e2;    v1=v2;
   e2=et;    v2=vt;
end
```

```
if  e1>e3
    et=e1;    vt=v1;
    e1=e3;    v1=v3;
    e3=et;    v3=vt;
end
if  e1>e4
    et=e1;    vt=v1;
    e1=e4;    v1=v4;
    e4=et;    v4=vt;
end
if  e2>e3
    et=e2;    vt=v2;
    e2=e3;    v2=v3;
    e3=et;    v3=vt;
end
if  e2>e4
    et=e2;    vt=v2;
    e2=e4;    v2=v4;
    e4=et;    v4=vt;
end
if  e3>e4
    et=e3;    vt=v3;
    e3=e4;    v3=v4;
    e4=et;    v4=vt;
end

% calculate and display the transition frequencies
f12=(e2-e1)/6.626e-18, f13=(e3-e1)/6.626e-18, f14=(e4-e1)/6.626e-18,
f23=(e3-e2)/6.626e-18, f24=(e4-e2)/6.626e-18, f34=(e4-e3)/6.626e-18,

% calculate and display the spin vectors
S12=[v2'*Sx*v1; v2'*Sy*v1; v2'*Sz*v1]
S13=[v3'*Sx*v1; v3'*Sy*v1; v3'*Sz*v1]
S14=[v4'*Sx*v1; v4'*Sy*v1; v4'*Sz*v1]
S23=[v3'*Sx*v2; v3'*Sy*v2; v3'*Sz*v2]
S24=[v4'*Sx*v2; v4'*Sy*v2; v4'*Sz*v2]
S34=[v4'*Sx*v3; v4'*Sy*v3; v4'*Sz*v3]

%display the "transition probabilities" for the rf signal
T12=(Hrf'*S12)*(Hrf'*S12)', T13=(Hrf'*S13)*(Hrf'*S13)',
T14=(Hrf'*S14)*(Hrf'*S14)', T23=(Hrf'*S23)*(Hrf'*S23)',
T24=(Hrf'*S24)*(Hrf'*S24)', T34=(Hrf'*S34)*(Hrf'*S34)',
```

The sample output follows. The user specifies the values of h, thetad, phid, and Hrf. The program determines the frequencies, spin vectors, and transition probabilities. The numbers 1,2,3,4 identify the quantum states, with 1 being the lowest energy state and 4 being the highest.

```
h = 4981
thetad = 90
phid = 0
Hrf =    0.8540
         0 - 0.5210i
         0
```

f12 = 8.4214
f13 = 24.0415
f14 = 43.2512
f23 = 15.6201
f24 = 34.8298
f34 = 19.2097

S12 = −1.0735
  0 + 0.6544i
  0

S13 = 0
  0
  0.4140

S14 = −0.0287
  0 + 0.0899i
  0

S23 = −0.9078
  0 + 1.0264i
  0

S24 = 0
  0
  0.2858

S34 = −0.7229
  0 + 1.0051i
  0

T12 = 1.5819
T13 = 0
T14 = 0.0051
T23 = 1.7160
T24 = 0
T34 = 1.3018

Appendix B
Derivation of the Hamiltonian Used in Equation (2)

The reader may be convinced of the equivalence of Eqs. (1) and (2) in the following way. First, Eq. (1) is expressed in spherical coordinates. This gives the result

$$H_s = g_1\beta H\cos\theta S_z + g_2\beta H(\sin\theta\cos\varphi S_x + \sin\theta\sin\varphi S_y) - D\left[S_z^2 - \frac{1}{3}S(S+1)\right] \tag{B-1}$$

Then the coordinate system is rotated three times. First the coordinate system is rotated about the z-axis by an angle φ until the static magnetic field is in the x'–z' plane. Then the coordinate system is rotated by an angle $-\theta$ about the y'-axis until the dc magnetic field is along the z''-direction. Finally, the coordinate system is rotated about the z''-axis by the angle $(\pi - \varphi)$. The rotation matrix relating the unprimed coordinates and the triple-primed coordinates is the product of the three rotation matrices:

$$\begin{bmatrix} x \\ y \\ z \end{bmatrix} = \begin{bmatrix} \cos\varphi & -\sin\varphi & 0 \\ \sin\varphi & \cos\varphi & 0 \\ 0 & 0 & 1 \end{bmatrix} \begin{bmatrix} \cos\theta & 0 & \sin\theta \\ 0 & 1 & 0 \\ -\sin\theta & 0 & \cos\theta \end{bmatrix} \begin{bmatrix} -\cos\varphi & -\sin\varphi & 0 \\ \sin\varphi & -\cos\varphi & 0 \\ 0 & 0 & 1 \end{bmatrix} \begin{bmatrix} x''' \\ y''' \\ z''' \end{bmatrix}$$

Now we use the rather remarkable fact that the spin matrices transform just like the components of a vector. Thus, the relationship between the unprimed spin operators and the triple-primed spin operators is the same as the above relationship between the coordinates. Thus, we can write

$$\begin{bmatrix} S_x \\ S_y \\ S_z \end{bmatrix} = \begin{bmatrix} -\cos\theta\cos^2\varphi - \sin^2\varphi & -\sin\varphi\cos\varphi\cos\theta + \sin\varphi\cos\varphi & \sin\theta\cos\varphi \\ -\cos\theta\sin\varphi\cos\varphi + \sin\varphi\cos\varphi & -\cos\theta\sin^2\varphi - \cos^2\varphi & \sin\theta\sin\varphi \\ \sin\theta\cos\varphi & \sin\theta\sin\varphi & \cos\theta \end{bmatrix} \begin{bmatrix} S_{x'''} \\ S_{y'''} \\ S_{z'''} \end{bmatrix}$$

Expressing the spin operators S_x, S_y, S_z in Eq. (B-1) in terms of $S_{x'''}, S_{y'''}, S_{z'''}$ leads to Eq. (2), where the triple primes have been dropped. Equation (2) neglects Zeeman terms involving differences between g_1 and g_2.